PHYSICAL REVIEW D **85,** 034036 (2012)

Direct *CP* violation in two-body hadronic charmed meson decays

Hai-Yang Cheng
Institute of Physics, Academia Sinica, Taipei, Taiwan 11529, Republic of China

Cheng-Wei Chiang
Department of Physics and Center for Mathematics and Theoretical Physics, National Central University, Chungli, Taiwan 32001, Republic of China
Institute of Physics, Academia Sinica, Taipei, Taiwan 11529, Republic of China

Physics Division, National Center for Theoretical Sciences, Hsinchu, Taiwan 30013, Republic of China
(Received 9 January 2012; published 22 February 2012)

Motivated by the recent observation of *CP* violation in the charm sector by LHCb, we study direct *CP* asymmetries in the standard model (SM) for the singly Cabibbo-suppressed two-body hadronic decays of charmed mesons using the topological-diagram approach. In this approach, the magnitude and the phase of topological weak annihilation amplitudes, which arise mainly from final-state rescattering, can be extracted from the data. Consequently, direct *CP* asymmetry $a_{\rm dir}^{\rm (tree)}$ at tree level can be *reliably* estimated. In general, it lies in the range $10^{-4} < a_{\rm dir}^{\rm (tree)} < 10^{-3}$. Short-distance QCD penguins and penguin annihilation are calculated using QCD factorization. Their effects are generally small, especially for $D \to VP$ modes. Since weak penguin annihilation receives long-distance contributions from the color-allowed tree amplitude followed by final-state rescattering, it is expected to give the dominant contribution to the direct *CP* violation in the decays $D^0 \to K^+K^-$ and $D^0 \to \pi^+\pi^-$, in which $a_{\rm dir}^{\rm (tree)}$ is absent. The maximal $\Delta a_{CP}^{\rm dir}$, the direct *CP* asymmetry difference between the above-mentioned two modes, allowed in the SM is around -0.25%, more than 2σ away from the current world average of $-(0.645 \pm 0.180)\%$.

DOI: 10.1103/PhysRevD.85.034036 PACS numbers: 14.40.Lb, 11.30.Er

I. INTRODUCTION

Recently the LHCb Collaboration has reported a result of a nonzero value for the difference between the time-integrated *CP* asymmetries of the decays $D^0 \to K^+K^-$ and $D^0 \to \pi^+\pi^-$ [1]

$$\Delta A_{CP} \equiv A_{CP}(K^+K^-) - A_{CP}(\pi^+\pi^-) = -(0.82 \pm 0.21 \pm 0.11)\% \quad \text{(LHCb)} \quad (1)$$

based on 0.62 fb^{-1} of 2011 data. The significance of the measured deviation from zero is 3.5σ. However, based on a data sample corresponding to the integrated luminosity of 5.9 fb^{-1}, the CDF Collaboration [2] obtained $A_{CP}(\pi^+\pi^-) = (0.22 \pm 0.24 \pm 0.11)\%$ and $A_{CP}(K^+K^-) = -(0.24 \pm 0.22 \pm 0.09)\%$, and hence

$$\Delta A_{CP} = -(0.46 \pm 0.31 \pm 0.11)\% \quad \text{(CDF)}. \quad (2)$$

The time-integrated asymmetry can be written to first order as

$$A_{CP}(f) = a_{CP}^{\rm dir}(f) + \frac{\langle t \rangle}{\tau} a_{CP}^{\rm ind}, \quad (3)$$

where $a_{CP}^{\rm dir}$ is the direct *CP* asymmetry, $a_{CP}^{\rm ind}$ is the indirect *CP* asymmetry, $\langle t \rangle$ is the average decay time in the sample, and τ is the D^0 lifetime. A global fit to the data of ΔA_{CP} is consistent with no *CP* violation only at 0.128% CL [3]. The central values and $\pm 1\sigma$ errors for the individual parameters are: $a_{CP}^{\rm ind} = -(0.019 \pm 0.232)\%$ and $\Delta a_{CP}^{\rm dir} = -(0.645 \pm 0.180)\%$.

Whether the first evidence of *CP* violation in the charm sector observed by LHCb is consistent with the standard model (SM) or implies new physics will require further analysis of more data and improved theoretical understanding. For some early and recent theoretical studies, see Refs. [4–12,12,13].

It is known that in order to induce direct *CP* violation, one needs at least two distinct decay amplitudes with nontrivial strong and weak phase differences. In *B* physics, there exist several QCD-inspired approaches describing the nonleptonic *B* decays, such as QCD factorization (QCDF) [14], pQCD [15], and soft collinear effective theory [16]. Even so, one needs to consider $1/m_b$ power corrections in order to explain the observed direct *CP* asymmetries in *B* decays. For example, in QCDF it is necessary to take into account two different types of power correction effects in order to resolve the *CP* puzzles and rate deficit problems with penguin-dominated two-body decays of *B* mesons and color-suppressed tree-dominated $\pi^0\pi^0$ and $\rho^0\pi^0$ modes: penguin annihilation and soft corrections to the color-suppressed tree amplitude [17].

The situation is far worse in the charm sector as a theoretical description of the underlying mechanism for exclusive hadronic *D* decays based on QCD is still not yet available. This is because the mass of the charmed quark, being of order 1.5 GeV, is not heavy enough to allow for a sensible heavy quark expansion. Indeed, it does not make too much sense to generalize the QCDF and pQCD

approaches to charm decays as the $1/m_c$ power corrections are so large that the heavy quark expansion is beyond control. In short, there is no reliable model which allows us to estimate the phases and magnitudes of the decay amplitudes beyond the color-allowed tree amplitude.

Luckily, we do have a powerful tool which provides a model-independent analysis of the charmed meson decays based on symmetry, namely, the diagrammatic approach. In this approach, the flavor-flow diagrams are classified according to the topologies of weak interactions with all strong interaction effects included. Based on flavor SU(3) symmetry, this model-independent analysis enables us to extract the topological amplitudes and probe the relative importance of different underlying decay mechanisms. It is complementary to the factorization approaches. Analysis based on the flavor-diagram approach indicates a sizable weak annihilation (W-exchange or W-annihilation) topological amplitude with a large strong phase relative to the tree amplitude. Since weak annihilation and final-state interactions (FSI's) are both of order $1/m_c$ in the heavy quark limit, this means FSI's could play an essential role in charm decays. Indeed, weak annihilation contributions arise mainly from final-state rescattering, and this explains why an approach based on heavy quark expansion in $1/m_c$ is not suitable for charm decays.

The great merit and the strong point of the topological-diagram approach is that the magnitude and the relative strong phase of each individual topological tree amplitude in charm decays can be extracted from the data.[1] This allows us to calculate CP asymmetry at tree level in a reliable way, granting us an idea about the size of CP violation in charmed meson decays.

Since there is no tree-level direct CP violation in $D^0 \to K^+K^-$ and $D^0 \to \pi^+\pi^-$ decays, the observation of ΔA_{CP} by LHCb indicates that, contrary to the conventional wisdom, penguin diagrams in singly Cabibbo-suppressed (SCS) decay channels do play a crucial role for CP violation even though they may not affect the branching fractions. Indeed, this observation is quite natural in the topological approach since, just as the enhancement in weak annihilation diagrams through FSI's, weak penguin annihilation (more specifically, the QCD-penguin exchange diagram to be introduced in the next section) also receives contributions from the color-allowed tree amplitude followed by final-state rescattering.

The time-integrated CP asymmetry receives indirect CP-violating contributions denoted by $a_{CP}^{\rm ind}$ through the D^0-$\bar{D}^0$ mixing. Such a mixing is governed by the mixing parameters $x \equiv (m_1 - m_2)/\Gamma$ and $y \equiv (\Gamma_1 - \Gamma_2)/(2\Gamma)$ for the mass eigenstates D_1 and D_2, where $m_{1,2}$ and $\Gamma_{1,2}$ are respective masses and decay widths and Γ is the average decay width. It is known that the short-distance contribution to the mixing parameters is very small [18], of order 10^{-6}. On the theoretical side, there are two approaches: the inclusive one relying on the $1/m_c$ expansion (see *e.g.*, Ref. [19] for a recent study), and the exclusive one with all final states summed over. In Ref. [20], only the SU(3) breaking effect in phase space was considered for the estimate of y. Consequently, the previous estimate of mixing parameters is subject to larger uncertainties. We believe that a better approach is to concentrate on two-body decays and rely more on data than on theory. This is because the measured two-body decays account for about 75% of hadronic rates of the D mesons. For PP and VP modes, data with good precision for Cabibbo-favored (CF) and SCS decays are now available. For as-yet unmeasured doubly Cabibbo-suppressed (DCS) modes, their rates can be determined from the diagrammatic approach. We obtained $x = (0.10 \pm 0.02)\%$ and $y = (0.36 \pm 0.26)\%$ from the PP and VP final states which account for nearly half of the hadronic width of D^0 [21]. It is conceivable that when all hadronic states are summed over, one could have $x \sim (0.2\text{–}0.4)\%$ and $y \sim (0.5\text{–}0.7)\%$. At any rate, indirect CP violation is suppressed by the smallness of the mixing parameters x and y and, moreover, it tends to cancel in the difference between K^+K^- and $\pi^+\pi^-$ final states.

There are also a lot of experimental efforts measuring direct CP asymmetries in D decays with 3-body and 4-body final states. This will involve a more complicated and time-consuming Dalitz-plot analysis. Nevertheless, the analysis will be very rewarding as it will provide us with much more information about the underlying mechanism for CP violation. We plan to explore this topic elsewhere.

The purpose of this work is to provide a realistic SM estimate of direct CP violation in two-body hadronic D decays based on the topological-diagram approach. In Sec. II we recapitulate the essence of the diagrammatic approach and its application to SCS $D \to PP$ and $D \to VP$ decays. The importance of final-state interactions is emphasized. The topological amplitudes are related to the quantities in the QCDF approach in Sec. III. Sec. IV is devoted to the calculation of direct CP asymmetries by taking into account SU(3) breaking and penguin effects. Sec. V contains our conclusions.

II. DIAGRAMMATIC APPROACH

A. Analysis for hadronic charm decays

It has been established some time ago that a least model-dependent analysis of heavy meson decays can be carried out in the so-called quark-diagram approach [22–24]. In this diagrammatic scenario, the topological diagrams can be classified into three distinct groups as follows (see Fig. 1):

(1) tree and penguin amplitudes:

(i) T, color-allowed external W-emission tree amplitude;

[1]This is not the case in B decays where one has to make additional assumptions in order to extract individual topological amplitude cleanly from the data.

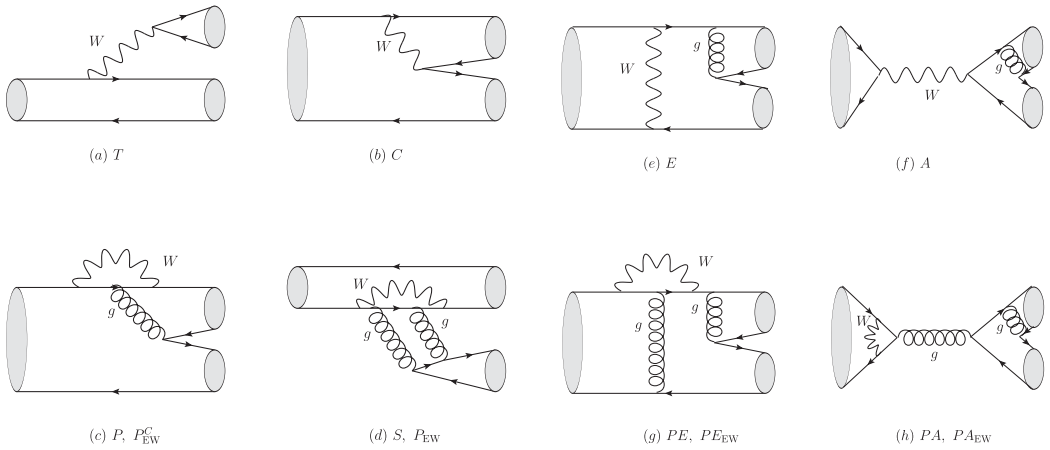

FIG. 1. Topology of possible flavor diagrams: (a) color-allowed tree T, (b) color-suppressed tree C, (c) QCD-penguin P, (d) singlet QCD-penguin S diagrams with 2 (3) gluon lines for M_2 being a pseudoscalar meson P (a vector meson V), where M_2 is generally the emitted meson or it contains a quark from the weak vertex for the annihilation diagram, (e) W-exchange E, (f) W-annihilation A, (g) QCD-penguin exchange PE, and (h) QCD-penguin annihilation PA diagrams. The color-suppressed EW-penguin $P^C_{\rm EW}$ and color-favored EW-penguin $P_{\rm EW}$ diagrams are obtained by replacing the gluon line from (c) and all the gluon lines from (d), respectively, by a single Z-boson or photon line. The EW-penguin exchange $PE_{\rm EW}$ and EW-penguin annihilation $PA_{\rm EW}$ diagrams are obtained from (g) and (h), respectively, by replacing the left gluon line by a single Z-boson or photon line. The gluon line of (e) and (f) and the right gluon line of (g) and (h) can be attached to the quark lines in all possible ways.

(ii) C, color-suppressed internal W-emission tree amplitude;
(iii) P, QCD-penguin amplitude;
(iv) S, singlet QCD-penguin amplitude involving $\mathrm{SU(3)_F}$-singlet mesons (e.g., $\eta^{(\prime)}$, ω, ϕ);
(v) $P_{\rm EW}$, color-favored EW-penguin amplitude; and
(vi) $P^C_{\rm EW}$, color-suppressed EW-penguin amplitude;
(2) weak annihilation amplitudes:
(i) E, W-exchange amplitude;
(ii) A, W-annihilation amplitude; (E and A are often jointly called "weak annihilation" amplitudes.)
(iii) PE, QCD-penguin exchange amplitude;
(iv) PA, QCD-penguin annihilation amplitude;
(v) $PE_{\rm EW}$, EW-penguin exchange amplitude; and
(vi) $PA_{\rm EW}$, EW-penguin annihilation amplitude; (PE and PA are also jointly called "weak penguin annihilation" amplitudes) and
(3) flavor-singlet weak annihilation amplitudes: all involving $\mathrm{SU(3)_F}$-singlet mesons,
(i) SE, singlet W-exchange amplitude;
(ii) SA, singlet W-annihilation amplitude;
(iii) SPE, singlet QCD-penguin exchange amplitude;
(iv) SPA, singlet QCD-penguin annihilation amplitude;
(v) $SPE_{\rm EW}$, singlet EW-penguin exchange amplitude; and
(vi) $SPA_{\rm EW}$, singlet EW-penguin annihilation amplitude.

The reader is referred to Ref. [25] for details.

It should be stressed that these diagrams are classified purely according to the topologies of weak interactions and flavor flows with all strong interaction effects encoded, and hence they are *not* Feynman graphs. All quark graphs used in this approach are topological and meant to include strong interactions to all orders, *i.e.*, gluon lines and quark loops are included implicitly in all possible ways. Therefore, analyses of topological graphs can provide information on FSI's.

The decomposition of the decay amplitudes of SCS $D \to PP$ and $D \to VP$ modes in terms of topological diagrams is displayed in Tables I and II. Since we will concentrate exclusively on SCS D decays, the primes on the amplitudes given in Ref. [28] are dropped. For simplicity, flavor-singlet weak annihilation and weak penguin annihilation amplitudes are neglected in these two tables.

The topological amplitudes T, C, E, A are extracted from the CF $D \to PP$ decays to be (in units of 10^{-6} GeV) [28] (see also [29])

$$T = 3.14 \pm 0.06, \quad C = (2.61 \pm 0.08)e^{-i(152\pm1)^\circ},$$
$$E = (1.53^{+0.07}_{-0.08})e^{i(122\pm2)^\circ}, \quad A = (0.39^{+0.13}_{-0.09})e^{i(31^{+20}_{-33})^\circ} \tag{4}$$

for $\phi = 40.4^\circ$ [30], where ϕ is the $\eta - \eta'$ mixing angle defined in the flavor basis

$$\begin{pmatrix} \eta \\ \eta' \end{pmatrix} = \begin{pmatrix} \cos\phi & -\sin\phi \\ \sin\phi & \cos\phi \end{pmatrix} \begin{pmatrix} \eta_q \\ \eta_s \end{pmatrix}, \tag{5}$$

with $\eta_q = \frac{1}{\sqrt{2}}(u\bar{u} + d\bar{d})$ and $\eta_s = s\bar{s}$.

For $D \to VP$ decays, there exist two different types of topological diagrams since the spectator quark of the charmed meson may end up in the pseudoscalar or vector meson. For reduced amplitudes T and C in $D \to VP$ decays, the subscript P (V) implies that the pseudoscalar (vector) meson contains the spectator quark of the charmed

TABLE I. Branching fractions and invariant amplitudes for singly Cabibbo-suppressed decays of charmed mesons to two pseudoscalar mesons. It is understood that the amplitudes with the CKM factor $\lambda_p \equiv V_{cp}^* V_{up}$ are summed over $p = d, s$. Data are taken from [26]. Predictions based on our best-fitted results in (4) with exact flavor SU(3) symmetry are given in the last column.

Mode		Representation	$\mathcal{B}_{\rm exp}$ ($\times 10^{-3}$)	$\mathcal{B}_{\rm theory}$ ($\times 10^{-3}$)
D^0	$\pi^+\pi^-$	$\lambda_p[(T+E)\delta_{pd} + P^p + PE + PA]$	1.400 ± 0.026	2.24 ± 0.10
	$\pi^0\pi^0$	$\frac{1}{\sqrt{2}}\lambda_p[(-C+E)\delta_{pd} + P^p + PE + PA)]$	0.80 ± 0.05	1.35 ± 0.05
	$\pi^0\eta$	$\lambda_p[-E\delta_{pd}\cos\phi - \frac{1}{\sqrt{2}}C\delta_{ps}\sin\phi + (P^p + PE)\cos\phi]$	0.68 ± 0.07	0.75 ± 0.02
	$\pi^0\eta'$	$\lambda_p[-E\delta_{pd}\sin\phi + \frac{1}{\sqrt{2}}C\delta_{ps}\cos\phi + (P^p + PE)\sin\phi]$	0.89 ± 0.14	0.74 ± 0.02
	$\eta\eta$	$\frac{1}{\sqrt{2}}\lambda_p\{[(C+E)\delta_{pd} + P^p + PE + PA]\cos^2\phi + (-\frac{1}{\sqrt{2}}C\sin 2\phi + 2E\sin^2\phi)\delta_{ps}\}$	1.67 ± 0.20	1.44 ± 0.08
	$\eta\eta'$	$\lambda_p\{\frac{1}{2}[(C+E)\delta_{pd} + P^p + PE + PA]\sin 2\phi + (\frac{1}{\sqrt{2}}C\cos 2\phi - E\sin 2\phi)\delta_{ps}\}$	1.05 ± 0.26	1.19 ± 0.07
	K^+K^-	$\lambda_p[(T+E)\delta_{ps} + P^p + PE + PA)]$	3.96 ± 0.08	1.92 ± 0.08
	$K^0\bar{K}^0$	$\lambda_p(E'_p + 2PA)$[a]	0.692 ± 0.116	0
D^+	$\pi^+\pi^0$	$\frac{1}{\sqrt{2}}\lambda_d(T+C)$	1.19 ± 0.06	0.88 ± 0.10
	$\pi^+\eta$	$\lambda_p[\frac{1}{\sqrt{2}}(T+C+2A)\delta_{pd}\cos\phi - C\delta_{ps}\sin\phi + \sqrt{2}(P^p + PE)\cos\phi]$	3.53 ± 0.21	1.48 ± 0.26
	$\pi^+\eta'$	$\lambda_p[\frac{1}{\sqrt{2}}(T+C+2A)\delta_{pd}\sin\phi + C\delta_{ps}\cos\phi + \sqrt{2}(P^p + PE)\sin\phi]$	4.67 ± 0.29	3.70 ± 0.37
	$K^+\bar{K}^0$	$\lambda_p[A\delta_{pd} + T\delta_{ps} + P^p + PE]$	5.66 ± 0.32	5.46 ± 0.53
D_s^+	π^+K^0	$\lambda_p[T\delta_{pd} + A\delta_{ps} + P^p + PE]$	2.42 ± 0.16	2.73 ± 0.26
	π^0K^+	$\frac{1}{\sqrt{2}}\lambda_p[-C\delta_{pd} + A\delta_{ps} + P^p + PE]$	0.62 ± 0.21	0.86 ± 0.09
	$K^+\eta$	$\frac{1}{\sqrt{2}}\lambda_p[C\delta_{pd} + A\delta_{ps} + P^p + PE]\cos\phi - \lambda_p[(T+C+A)\delta_{ps} + P^p + PE]\sin\phi$	1.75 ± 0.35	0.78 ± 0.09
	$K^+\eta'$	$\frac{1}{\sqrt{2}}\lambda_p[C\delta_{pd} + A\delta_{ps} + P^p + PE]\sin\phi + \lambda_p[(T+C+A)\delta_{ps} + P^p + PE]\cos\phi$	1.8 ± 0.6	1.07 ± 0.17

[a]The subscript p in E'_p refers to the quark-antiquark pair popping out of the vacuum in the final state.

meson. For E and A amplitudes with the final state $q_1\bar{q}_2$, the subscript P (V) denotes that the pseudoscalar (vector) meson contains the antiquark $\bar{q}_2$.

There are two different ways of extracting topological amplitudes: either

$$\Gamma(D \to VP) = \frac{p_c}{8\pi m_D^2}\sum_{\rm pol.}|\mathcal{A}|^2 \tag{6}$$

by summing over the polarization states of the vector meson, or through the relation

$$\Gamma(D \to VP) = \frac{p_c^3}{8\pi m_D^2}|\tilde{\mathcal{A}}|^2, \tag{7}$$

by taking the polarization vector out of the amplitude, where $\mathcal{A} = (m_V/m_D)\tilde{\mathcal{A}}(\varepsilon \cdot p_D)$. There exist two solutions, denoted by (A) and (S), for the T_V, C_P, and E_P amplitudes, depending on whether Eq. (6) or Eq. (7) is used to extract the invariant amplitudes. Assuming that T_P and T_V are relatively real, we obtain two best solutions (A1) and (S1) for T_P, C_V, and E_V [28] (see also Ref. [31])

$$\begin{aligned}
&(A)\ T_V = 4.16^{+0.16}_{-0.17}, && C_P = (5.14^{+0.30}_{-0.33})e^{i(162\pm3)^\circ}, && E_P = (3.09 \pm 0.11)e^{-i(93\pm5)^\circ},\\
&(S)\ T_V = 2.15^{+0.08}_{-0.09}, && C_P = (2.68^{+0.14}_{-0.15})e^{i(164\pm3)^\circ}, && E_P = (1.69 \pm 0.06)e^{-i(103\pm4)^\circ},\\
&(A1)\ T_P = 8.11^{+0.32}_{-0.43}, && C_V = (4.15^{+0.34}_{-0.57})e^{i(164^{+36}_{-10})^\circ}, && E_V = (1.51^{+0.97}_{-0.69})e^{-i(124^{+57}_{-26})^\circ},\\
&(S1)\ T_P = 3.14^{+0.31}_{-0.50}, && C_V = (1.33^{+0.36}_{-0.51})e^{i(177^{+16}_{-13})^\circ}, && E_V = (1.31^{+0.40}_{-0.47})e^{-i(106^{+13}_{-16})^\circ}.
\end{aligned} \tag{8}$$

Solutions (A) and (A1) in units of 10^{-6} are obtained using Eq. (7), while solutions (S) and (S1) in units of $10^{-6}(\varepsilon \cdot p_D)$ are extracted using Eq. (6). Note that all solutions are extracted from the CF $D \to VP$ decays and that the A_P and A_V amplitudes cannot be completely determined based on currently available data [28].

Under the flavor SU(3) symmetry, one can use the topological amplitudes extracted from the CF modes to predict the rates for the SCS and DCS decays. The branching fractions of SCS $D \to PP$ decays predicted in this way are shown in the last column of Table I. In general, the agreement with experiment is good except for discrepancies in some modes. For example, the predicted rates for $\pi^+\pi^-$ and $\pi^0\pi^0$ are too large, while those for K^+K^-, $\pi^+\eta^{(\prime)}$, and $K^+\eta^{(\prime)}$ are too small compared to experiments. The decay $D^0 \to K^0\bar{K}^0$ is prohibited by the SU(3) symmetry, but the measured rate is comparable to that of $D^0 \to \pi^0\pi^0$.

TABLE II. Same as Table I except for singly Cabibbo-suppressed decays of charmed mesons to one vector and one pseudoscalar mesons. Because of the lack of information on A_P and A_V, no prediction is attempted for D^+ and D_s^+ decays except $D^+ \to \pi^+\phi$.

Mode		Representation	$\mathcal{B}_{\text{exp}}$ ($\times 10^{-3}$)	$\mathcal{B}_{\text{theory}}$ (A, A1) ($\times 10^{-3}$)	$\mathcal{B}_{\text{theory}}$ (S, S1) ($\times 10^{-3}$)
D^0	$\pi^+\rho^-$	$\lambda_p[(T_V + E_P)\delta_{pd} + P_V^p + PA_P + PE_P]$	4.96 ± 0.24	3.92 ± 0.46	5.18 ± 0.58
	$\pi^-\rho^+$	$\lambda_p[(T_P + E_V)\delta_{pd} + P_P^p + PA_V + PE_V]$	9.8 ± 0.4	8.34 ± 1.69	8.27 ± 1.79
	$\pi^0\rho^0$	$\frac{1}{2}\lambda_p[(-C_P - C_V + E_P + E_V)\delta_{pd} + P_P^p + P_V^p + PA_P + PA_V + PE_P + PE_V]$	3.72 ± 0.22	2.96 ± 0.98	3.34 ± 0.33
	K^+K^{*-}	$\lambda_p[(T_V + E_P)\delta_{ps} + P_V^p + PE_P + PA_P]$	1.56 ± 0.12	1.99 ± 0.24	1.99 ± 0.22
	K^-K^{*+}	$\lambda_p[(T_P + E_V)\delta_{ps} + P_P^p + PE_V + PA_V]$	4.38 ± 0.21	4.25 ± 0.86	3.18 ± 0.69
	$K^0\bar{K}^{*0}$	$\lambda_p(E_V\delta_{pd} + E_P\delta_{ps} + PA_P + PA_V)$	<1.5	0.29 ± 0.22	0.05 ± 0.06
	$\bar{K}^0K^{*0}$	$\lambda_p(E_P\delta_{pd} + E_V\delta_{ps} + PA_P + PA_V)$	<0.84	0.29 ± 0.22	0.05 ± 0.06
	$\pi^0\omega$	$\frac{1}{2}\lambda_p[(-C_V + C_P - E_P - E_V)\delta_{pd} + P_P^p + P_V^p + PE_P + PE_V]$	<0.26	0.10 ± 0.18	1.01 ± 0.18
	$\pi^0\phi$	$\frac{1}{\sqrt{2}}\lambda_s C_P$	1.31 ± 0.17	1.22 ± 0.08	1.11 ± 0.05
	$\eta\omega$	$\frac{1}{2}\lambda_p[(C_V + C_P + E_V + E_P)\delta_{pd}\cos\phi - C_V\delta_{ps}\sin\phi + (P_P^p + P_V^p + PE_P + PE_V + PA_P + PA_V)\cos\phi]$	2.21 ± 0.23[a]	3.08 ± 1.42	3.94 ± 0.61
	$\eta'\omega$	$\frac{1}{2}\lambda_p[(C_V + C_P + E_V + E_P)\delta_{pd}\sin\phi + C_V\delta_{ps}\cos\phi + (P_P^p + P_V^p + PE_P + PE_V + PA_P + PA_V)\sin\phi]$	-	0.07 ± 0.02	0.15 ± 0.01
	$\eta\phi$	$\lambda_p\{[\frac{1}{\sqrt{2}}C_P\cos\phi - (E_V + E_P)\sin\phi]\delta_{ps} + (PA_P + PA_V)\sin\phi\}$	0.14 ± 0.05	0.31 ± 0.10	0.41 ± 0.08
	$\eta\rho^0$	$\frac{1}{2}\lambda_p[(C_V - C_P - E_V - E_P)\delta_{pd}\cos\phi - \sqrt{2}C_V\delta_{ps}\sin\phi + (P_P^p + P_V^p + PE_P + PE_V)\cos\phi]$	-	1.11 ± 0.86	1.17 ± 0.34
	$\eta'\rho^0$	$\frac{1}{2}\lambda_p[(C_V - C_P - E_V - E_P)\delta_{pd}\sin\phi + \sqrt{2}C_V\delta_{ps}\cos\phi + (P_P^p + P_V^p + PE_P + PE_V)\sin\phi]$	-	0.14 ± 0.02	0.26 ± 0.02
D^+	$\pi^+\rho^0$	$\frac{1}{\sqrt{2}}\lambda_p[(T_V + C_P - A_P + A_V)\delta_{pd} + P_V^p - P_P^p + PE_P - PE_V]$	0.81 ± 0.15		
	$\pi^0\rho^+$	$\frac{1}{\sqrt{2}}\lambda_p[(T_P + C_V + A_P - A_V)\delta_{pd} + P_P^p - P_V^p + PE_V - PE_P]$	-		
	$\pi^+\omega$	$\frac{1}{\sqrt{2}}\lambda_p[(T_V + C_P + A_P + A_V)\delta_{pd} + P_P^p + P_V^p + PE_P + PE_V]$	<0.34		
	$\pi^+\phi$	$\lambda_s C_P$	$5.42^{+0.16}_{-0.18}$	6.21 ± 0.43	5.68 ± 0.28
	$\eta\rho^+$	$\frac{1}{\sqrt{2}}\lambda_p[(T_P + C_V + A_V + A_P)\delta_{pd}\cos\phi - \sqrt{2}C_V\delta_{ps}\sin\phi + (P_P^p + P_V^p + PE_P + PE_V)\cos\phi]$			
	$\eta'\rho^+$	$\frac{1}{\sqrt{2}}\lambda_p[(T_P + C_V + A_V + A_P)\delta_{pd}\sin\phi + \sqrt{2}C_V\delta_{ps}\cos\phi + (P_P^p + P_V^p + PE_P + PE_V)\sin\phi]$			
	$K^+\bar{K}^{*0}$	$\lambda_p(A_V\delta_{pd} + T_V\delta_{ps} + P_V^p + PE_P)$	$3.68^{+0.14}_{-0.21}$		
	$\bar{K}^0K^{*+}$	$\lambda_p(A_P\delta_{pd} + T_P\delta_{ps} + P_P^p + PE_V)$	32 ± 14		
D_s^+	π^+K^{*0}	$\lambda_p(T_V\delta_{pd} + A_V\delta_{ps} + P_V^p + PE_P)$	2.25 ± 0.39		
	π^0K^{*+}	$\frac{1}{\sqrt{2}}\lambda_p[C_V\delta_{pd} - A_V\delta_{ps} - P_V^p - PE_P]$	-		
	$K^+\rho^0$	$\frac{1}{\sqrt{2}}\lambda_p[C_P\delta_{pd} - A_P\delta_{ps} - P_P^p - PE_V]$	2.7 ± 0.5		
	$K^0\rho^+$	$\lambda_p(T_P\delta_{pd} + A_P\delta_{ps} + P_P^p + PE_V)$	-		
	ηK^{*+}	$\frac{1}{\sqrt{2}}\lambda_p\{(C_V\delta_{pd} + A_V\delta_{ps} + P_V^p + PE_P)\cos\phi - [(T_P + C_V + A_P)\delta_{ps} + P_P^p + PE_V]\sin\phi\}$	-		
	$\eta' K^{*+}$	$\frac{1}{\sqrt{2}}\lambda_p\{(C_V\delta_{pd} + A_V\delta_{ps} + P_V^p + PE_P)\sin\phi - [(T_P + C_V + A_P)\delta_{ps} + P_P^p + PE_V]\cos\phi\}$	-		
	$K^+\omega$	$\frac{1}{\sqrt{2}}\lambda_p[C_P\delta_{pd} + A_P\delta_{ps} + P_P^p + PE_V]$	<2.4		
	$K^+\phi$	$\lambda_p[(T_V + C_P + A_V)\delta_{ps} + P_V^p + PE_P]$	<0.6		

[a]Data from [27].

Some Cabibbo-suppressed modes exhibit sizable violation of flavor SU(3) symmetry. We find that part of the SU(3) breaking effects can be accounted for by SU(3) symmetry violation manifested in the color-allowed and color-suppressed tree amplitudes. However, in other cases such as the ratio $R \equiv \Gamma(D^0 \to K^+K^-)/\Gamma(D^0 \to \pi^+\pi^-)$, SU(3) breaking in spectator amplitudes is not sufficient to explain the observed value of R. This calls for the consideration of SU(3) violation in the W-exchange amplitudes.

B. Final-state rescattering

From Eq. (4) we see that the color-suppressed amplitude C is not only comparable to the tree amplitude T in magnitude but also has a large strong phase relative to T. (It is 180° in naive factorization.) The W-exchange E is sizable with a large phase of order 120°. Since W-exchange is of order $1/m_c$ in the heavy quark limit, this means that $1/m_c$ corrections are very important in charm decays. Finally, we see that W-annihilation is substantially smaller than W-exchange and almost perpendicular to E.

In naive factorization, the factorizable weak annihilation amplitudes are usually assumed to be negligible as they are helicity suppressed or, equivalently, the form factors are suppressed at large $q^2 = m_D^2$. At first glance, it appears that the factorizable weak annihilation amplitudes are too small to be consistent with experiments at all. However, in the diagrammatic approach here, the topological amplitudes E and A do receive contributions from the tree and color-suppressed amplitudes T and C, respectively, via final-state rescattering (see, e.g., Fig. 1 of Ref. [28]). Therefore, even if the short-distance weak annihilation vanishes, long-distance weak annihilation can be induced via inelastic FSI's.

For $D \to PP$ decays, it is expected that the long-distance W-exchange is dominated by resonant FSI's as shown in Fig. 1(a) of Ref. [28] owing to the fact that an abundant spectrum of resonances is known to exist at energies close to the mass of the charmed meson. It is easy to draw the relevant diagrams, but the difficulty is how to calculate them. In principle, one can evaluate the final-state rescattering contribution at the hadron level (see, e.g., Fig. 5 of Ref. [28]), but it involves many theoretical uncertainties. As stressed in the Introduction section, a great merit of the diagrammatic approach is that the magnitude and phase of the topological W-exchange and W-annihilation amplitudes can be extracted from the data [see Eq. (4)]. Moreover, the large magnitude and phase of weak annihilation can be quantitatively and qualitatively understood in the following manner. As emphasized in Refs. [32,33], most of the properties of resonances follow from unitarity alone, without regard to the dynamical mechanism that produces the resonances. Consequently, as shown in Refs. [32,34], the effect of resonance-induced FSI's can be described in a model-independent manner in terms of the mass and width of the nearby resonances. It is found that the E and A amplitudes are modified by resonant FSI's as (see, *e.g.*, Ref. [34])

$$\begin{aligned} E &= e + (e^{2i\delta_r} - 1)\left(e + \frac{T}{3}\right), \\ A &= a + (a^{2i\delta_r} - 1)\left(a + \frac{C}{3}\right), \end{aligned} \tag{9}$$

with

$$e^{2i\delta_r} = 1 - i\frac{\Gamma}{m_D - m_R + i\Gamma/2}, \tag{10}$$

where the W-exchange amplitude E and W-annihilation amplitude A before the resonant FSI's are denoted by e and a, respectively. Therefore, even if the short-distance weak annihilation is turned off, a long-distance W-exchange (W-annihilation) contribution can still be induced from the tree amplitude T (C) via FSI rescattering in resonance formation. To see the importance of resonant FSI's, consider the scalar resonance $K_0^*(1950)$ with a mass $1945 \pm 10 \pm 20$ MeV and a width $201 \pm 34 \pm 79$ MeV, contributing to the W-exchange in $D \to K\pi, K\eta$. Assuming $e = 0$ in Eq. (9), we obtain $E = 1.68 \times 10^{-6}\exp(i143°)$ GeV, which is close to the "experimental" value of E given in Eq. (4). This suggests that weak annihilation topologies in $D \to PP$ decays are dominated by nearby resonances via final-state rescattering. Contrary to the PP sector, we have shown in Ref. [28] that weak annihilation in VP systems is dominated by final-state rescattering via quark exchange.

III. TOPOLOGICAL AMPLITUDES AND QCD FACTORIZATION

Although the topological tree amplitudes T, C, E and A for hadronic D decays can be extracted from the data, we still need information on penguin amplitudes (QCD penguin, penguin annihilation, etc.) in order to estimate CP violation in the SCS decays. To calculate the penguin effect, we start from the short-distance effective Hamiltonian

$$\mathcal{H}_{\rm eff} = \frac{G_F}{\sqrt{2}}\left[\sum_{p=d,s}\lambda_p(c_1O_1^p + c_2O_2^p + c_{8g}O_{8g}) - \lambda_b\sum_{i=3}^{6}c_iO_i\right], \tag{11}$$

where $\lambda_p \equiv V_{cp}^*V_{up}$ for $p = d$, s, b, and

$$\begin{aligned} O_1^p &= (\bar{p}c)_{V-A}(\bar{u}p)_{V-A}, \\ O_2^p &= (\bar{p}_\alpha c_\beta)_{V-A}(\bar{u}_\beta p_\alpha)_{V-A}, \\ O_{3(5)} &= (\bar{u}c)_{V-A}\sum_q(\bar{q}q)_{V\mp A}, \\ O_{4(6)} &= (\bar{u}_\alpha c_\beta)_{V-A}\sum_q(\bar{q}_\beta q_\alpha)_{V\mp A}, \\ O_{8g} &= -\frac{g_s}{8\pi^2}m_c\bar{u}\sigma_{\mu\nu}(1+\gamma_5)G^{\mu\nu}c, \end{aligned} \tag{12}$$

with O_3-O_6 being the QCD-penguin operators and $(\bar{q}_1 q_2)_{V\pm A} \equiv \bar{q}_1 \gamma_\mu (1 \pm \gamma_5) q_2$. The electroweak penguin operators are not included in the Hamiltonian as they can be neglected in practice. For the Wilson coefficients, we take $c_1 = 1.21$, $c_2 = -0.41$, $c_3 = 0.02$, $c_4 = -0.04$, $c_5 = 0.01$, $c_6 = -0.05$, and $c_{8g} = -0.06$ from Ref. [7] evaluated at the scale $\mu = m_c$.

To evaluate the hadronic matrix elements of the 4-quark operators, it is necessary to specify a suitable framework for the task. We will work with the QCDF approach [14,35]. As shown in details in Ref. [25], various topological amplitudes of $D \to M_1 M_2$ decays can be expressed in terms of the quantities calculated in the framework of QCDF as follows:

$$\begin{aligned}
T &= \frac{G_F}{\sqrt{2}} a_1(M_1M_2) X^{(DM_1,M_2)},\\
C &= \frac{G_F}{\sqrt{2}} a_2(M_1M_2) X^{(DM_1,M_2)},\\
E &= \frac{G_F}{\sqrt{2}} (i f_D f_{M_1} f_{M_2})[b_1]_{M_1M_2},\\
A &= \frac{G_F}{\sqrt{2}} (i f_D f_{M_1} f_{M_2})[b_2]_{M_1M_2},\\
P^p &= \frac{G_F}{\sqrt{2}} [a_4^p(M_1M_2) + \eta r_\chi^{M_2} a_6^p(M_1M_2)] X^{(DM_1,M_2)},\\
PE &= \frac{G_F}{\sqrt{2}} (i f_D f_{M_1} f_{M_2})[b_3]_{M_1M_2},\\
PA &= \frac{G_F}{\sqrt{2}} (i f_D f_{M_1} f_{M_2})[b_4]_{M_1M_2},
\end{aligned} \tag{13}$$

where $\eta = 1$ for $M_1M_2 = PP$, PV and $\eta = -1$ for $M_1M_2 = VP$. In the above equations, the quantities b_i with $i = 1, \cdots, 4$ expressed in terms of annihilation amplitudes are defined in Ref. [35], and X is a factorizable matrix element given by

$$\begin{aligned}
X^{(DP_1,P_2)} &\equiv \langle P_2|J^\mu|0\rangle\langle P_1|J'_\mu|D\rangle\\
&= i f_{P_2}(m_D^2 - m_{P_1}^2) F_0^{DP_1}(m_{P_2}^2),\\
X^{(DP,V)} &\equiv \langle V|J^\mu|0\rangle\langle P|J'_\mu|D\rangle = 2 f_V m_D p_c F_1^{DP}(m_V^2),\\
X^{(DV,P)} &\equiv \langle P|J^\mu|0\rangle\langle V|J'_\mu|D\rangle = 2 f_P m_D p_c A_0^{DV}(m_P^2),
\end{aligned} \tag{14}$$

with p_c being the center-of-mass momentum of either final-state particle. Here we have followed the conventional Bauer-Stech-Wirbel definition for form factors $F_{0,1}^{DP}$ and A_0^{DV} [36]. For annihilation amplitudes, we choose the convention that M_1 (M_2) contains an antiquark (a quark) from the weak vertex. The chiral factors $r_\chi^{M_2}$ in Eq. (13) are given by

$$r_\chi^P(\mu) = \frac{2m_P^2}{m_c(\mu)(m_2 + m_1)(\mu)}, \quad r_\chi^V(\mu) = \frac{2m_V}{m_c(\mu)} \frac{f_V^\perp(\mu)}{f_V}, \tag{15}$$

with $f_V^\perp(\mu)$ being the scale-dependent transverse decay constant of the vector meson V. The flavor operators a_i^p in Eq. (13) are basically the Wilson coefficients in conjunction with short-distance nonfactorizable corrections such as vertex corrections and hard spectator interactions. In general, they have the expressions [35]

$$\begin{aligned}
a_i^p(M_1M_2) = &\left(c_i + \frac{c_{i\pm1}}{N_c}\right) N_i(M_2) + \frac{c_{i\pm1}}{N_c} \frac{C_F \alpha_s}{4\pi} \left[V_i(M_2) \right.\\
&\left. + \frac{4\pi^2}{N_c} H_i(M_1M_2) \right] + \mathcal{P}_i^p(M_2),
\end{aligned} \tag{16}$$

where $i = 1, \cdots, 10$, the upper (lower) signs apply when i is odd (even), c_i are the Wilson coefficients, $C_F = (N_c^2 - 1)/(2N_c)$ with $N_c = 3$, M_2 is the emitted meson, and M_1 shares the same spectator quark as the D meson. The quantities $V_i(M_2)$ account for vertex corrections, $H_i(M_1M_2)$ for hard spectator interactions with a hard gluon exchange between the emitted meson and the spectator quark of the D meson, and $\mathcal{P}_i(M_2)$ for penguin contractions. The explicit expressions of V_i, H_i, and $\mathcal{P}_i$ can be found in Ref. [35]. The quantities $N_i(M_2)$ vanish when $i = 6, 8$ and $M_2 = V$, and are equal to unity otherwise.

In general, the decay amplitude is evaluated at the scale $\mu = m_c(m_c)$. However, as stressed in Ref. [14], the hard spectator and annihilation contributions should be evaluated at the hard-collinear scale $\mu_h = \sqrt{\mu \Lambda_h}$ with $\Lambda_h \approx 500$ MeV. This means $\mu_h \approx 0.8$ GeV for $D \to M_1 M_2$ decays, which is beyond the regime where perturbative QCD is applicable. Therefore, we shall not consider the spectator contributions to a_i.

Let us first consider the penguin amplitude

$$P_{\pi\pi}^p = \frac{G_F}{\sqrt{2}} [a_4^p(\pi\pi) + r_\chi^\pi a_6^p(\pi\pi)] X^{(D\pi,\pi)}, \tag{17}$$

with

$$\begin{aligned}
a_4^p(\pi\pi) &= \left(c_4 + \frac{c_3}{N_c}\right) + \frac{c_3}{N_c} \frac{C_F \alpha_s}{4\pi} \left[V_4^p + \frac{4\pi^2}{N_c} H_4^p \right] + \mathcal{P}_4^p,\\
a_6^p(\pi\pi) &= \left(c_6 + \frac{c_5}{N_c}\right) + \frac{c_5}{N_c} \frac{C_F \alpha_s}{4\pi} \left[V_6^p + \frac{4\pi^2}{N_c} H_6^p \right] + \mathcal{P}_6^p.
\end{aligned} \tag{18}$$

The strong phase of the QCD-penguin amplitude arises from vertex corrections and penguin contractions. The order α_s corrections from penguin contraction read [35]

$$\mathcal{P}_4^p = \frac{C_F\alpha_s}{4\pi N_c}\left\{c_1\left[\frac{4}{3}\ln\frac{m_c}{\mu}+\frac{2}{3}-G_{M_2}(s_p)\right]+c_3\left[\frac{8}{3}\ln\frac{m_c}{\mu}+\frac{4}{3}-G_{M_2}(s_u)-G_{M_2}(1)\right]\right.$$
$$\left.+(c_4+c_6)\left[\frac{16}{3}\ln\frac{m_c}{\mu}-G_{M_2}(s_u)-G_{M_2}(s_d)-G_{M_2}(s_s)-G_{M_2}(1)\right]\right\},$$
$$\mathcal{P}_6^p = \frac{C_F\alpha_s}{4\pi N_c}\left\{c_1\left[\frac{4}{3}\ln\frac{m_c}{\mu}+\frac{2}{3}-\hat{G}_{M_2}(s_p)\right]+c_3\left[\frac{8}{3}\ln\frac{m_c}{\mu}+\frac{4}{3}-\hat{G}_{M_2}(s_u)-\hat{G}_{M_2}(1)\right]\right.$$
$$\left.+(c_4+c_6)\left[\frac{16}{3}\ln\frac{m_c}{\mu}-\hat{G}_{M_2}(s_u)-\hat{G}_{M_2}(s_d)-\hat{G}_{M_2}(s_s)-\hat{G}_{M_2}(1)\right]\right\}, \quad (19)$$

where $s_i = m_i^2/m_c^2$,

$$G_{M_2}(s) = \int_0^1 dx G(s,1-x)\Phi_{M_2}(x),$$
$$\hat{G}_{M_2}(s) = \int_0^1 dx G(s,1-x)\Phi_{m_2}(x), \quad (20)$$

and $G(s,x) = -4\int_0^1 duu(1-u)\ln[s-u(1-u)x]$. Here Φ_{M_2} (Φ_{m_2}) is the twist-2 (-3) light-cone distribution amplitude for the meson M_2.

Weak points of QCD-inspired approaches

Although QCD-inspired approaches such as pQCD [37] and QCDF [38–42] have been applied to charm decays, their results cannot be taken seriously. Since the charm quark mass is not heavy enough, the $1/m_c$ power corrections are so large that a sensible heavy quark expansion is not allowed. The large magnitude and phase of weak annihilation (E or A) topological amplitude, which is of order $1/m_c$ in heavy quark limit, is an indicative of the importance of power corrections in charm decays. For the parameters a_1 and a_2 in $D^0 \to K^-\pi^+$ decays, we find

$$a_1(\bar{K}\pi) = 1.19e^{i2.6^\circ}, \qquad a_2(\bar{K}\pi) = 0.37e^{-i155^\circ}, \quad (21)$$

where the strong phases arise from the vertex correction. In Ref. [28], we have shown that for $D \to \bar{K}\pi$ decays

$$|a_1| = 1.22 \pm 0.02, \qquad |a_2| = 0.82 \pm 0.02,$$
$$a_2/a_1 = (0.67 \pm 0.02)e^{-i(152\pm1)^\circ}, \quad (22)$$

as obtained from the topological amplitudes T and C given in Eq. (4). It is clear that, while the calculated a_1 is consistent with "experiment", the predicted a_2 in QCDF is too small in magnitude and this again calls for large $1/m_c$ corrections.

While there is no trustworthy theoretical framework for describing the hadronic D decays, in this work we shall use the NLO predictions of QCDF to give a crude estimate of the short-distance penguin contributions.

IV. DIRECT CP VIOLATION

A. Tree-level CP violation

Direct CP asymmetry in hadronic charm decays defined by

$$a_{CP}^{\rm dir}(f) = \frac{\Gamma(D\to f)-\Gamma(\bar{D}\to\bar{f})}{\Gamma(D\to f)+\Gamma(\bar{D}\to\bar{f})} \quad (23)$$

can occur even at the tree level [43]. Take the $D_s^+ \to K^0\pi^+$ mode as an example. Its decay amplitude reads $\lambda_d(T+P^d+PE)+\lambda_s(A+P^s+PE)$ (see Table I). The interference between the color-allowed tree and W-annihilation amplitudes leads to the tree-level CP asymmetry

$$a_{\rm dir}^{\rm (tree)}(D_s^+\to K^0\pi^+) = \frac{2{\rm Im}(\lambda_d\lambda_s^*)}{|\lambda_d|^2}\frac{{\rm Im}(T^*A)}{|T-A|^2}$$
$$\approx 1.2\times10^{-3}\left|\frac{A}{T}\right|\sin\delta_{AT}, \quad (24)$$

where δ_{AT} is the strong phase of A relative to T and we have taken into account the fact that the magnitude of A is much smaller than T. It is obvious that direct CP violation in charm decays is CKM suppressed by a factor of 10^{-3}. Assuming the same topological amplitudes in SCS and CF decays, we then find from Eqs. (4) and (24) that $a_{\rm dir}^{\rm (tree)} \approx 10^{-4}$ for $D_s^+\to K^0\pi^+$. Larger direct CP asymmetry can be achieved in those decay modes with interference between T and C or C and E. For example, $a_{\rm dir}^{\rm (tree)}$ is of order -1.1×10^{-3} for $D^0\to\omega\eta'$ and of order $(0.6\text{–}0.7)\times10^{-3}$ for $D^0\to\pi^0\eta$ and $D^0\to K^0\bar{K}^{*0}$.

B. Penguin-induced CP violation

Direct CP violation does not occur at the tree level in some of the SCS decays, such as $D^0\to K^+K^-$ and $D^0\to\pi^+\pi^-$. In these two decays, the CP asymmetry can only arise from the interference between tree and penguin amplitudes

$$a_{\rm dir}^{\rm (loop)}(\pi^+\pi^-) = \frac{2{\rm Im}(\lambda_d\lambda_s^*)}{|\lambda_d|^2}$$
$$\times\frac{{\rm Im}[(T^*+E^*+P^{d*}+PE+PA)(P^s+PE+PA)]_{\pi\pi}}{|T_{\pi\pi}+E_{\pi\pi}|^2}$$
$$\approx 1.2\times10^{-3}\left|\frac{P^s+PE+PA}{T+E}\right|_{\pi\pi}\sin\delta_{\pi\pi}, \quad (25)$$

where $\delta_{\pi\pi}$ is the strong phase of $P^s_{\pi\pi}+PE_{\pi\pi}+PA_{\pi\pi}$ relative to $T_{\pi\pi}+E_{\pi\pi}$. Likewise,

$$a_{\rm dir}^{\rm (loop)}(K^+K^-) \approx -1.2\times 10^{-3}\left|\frac{P^d+PE+PA}{T+E}\right|_{KK}\sin\delta_{KK}. \quad (26)$$

To estimate their *CP* asymmetries, we first discuss the rates of $D^0\to\pi^+\pi^-$ and $D^0\to K^+K^-$. Experimentally, the ratio $R\equiv\Gamma(D^0\to K^+K^-)/\Gamma(D^0\to\pi^+\pi^-)$ is about 2.8 [26], while it should be unity in the SU(3) limit. This is a long-standing puzzle since SU(3) symmetry is expected to be broken at the level of 30% only. Without the inclusion of SU(3) breaking effects in the topological amplitudes, we see from Table I that the predicted rate of K^+K^- is even smaller than that of $\pi^+\pi^-$ due to less phase space available to the former. In the factorization approach, SU(3)-breaking effects in the tree amplitudes T are given by

$$\frac{T_{KK}}{T}=\frac{f_K}{f_\pi}\frac{F_0^{DK}(m_K^2)}{F_0^{DK}(m_\pi^2)},\quad \frac{T_{\pi\pi}}{T}=\frac{m_D^2-m_\pi^2}{m_D^2-m_K^2}\frac{F_0^{D\pi}(m_\pi^2)}{F_0^{DK}(m_\pi^2)}. \quad (27)$$

Using the form factor q^2 dependence and input parameters given in Ref. [28], we obtain

$$T_{KK}/T=1.275,\qquad T_{\pi\pi}/T=0.96. \quad (28)$$

This leads to $\mathcal{B}(D^0\to K^+K^-)=(3.4\pm0.1)\times10^{-3}$ and $\mathcal{B}(D^0\to\pi^+\pi^-)=(2.1\pm0.1)\times10^{-3}$ assuming no SU(3) symmetry breaking in E, i.e., $E_{KK}=E_{\pi\pi}=E$. Therefore, SU(3) breaking in spectator amplitudes leads to $R=1.6$ and is still not sufficient to explain the observed value of $R\approx2.8$. This calls for the consideration of flavor symmetry SU(3) violation in the W-exchange amplitudes. We have argued in Ref. [28] that the long-distance resonant contribution through the nearby state $f_0(1710)$ could account for SU(3)-breaking effects in the W-exchange topology. This has to do with the dominance of the scalar glueball content of $f_0(1710)$ and the chiral suppression effect in the ratio $\Gamma(f_0(1710)\to\pi\bar\pi)/\Gamma(f_0(1710)\to K\bar K)$. To fit the measured branching fractions we find

$$E_{KK}=1.6\times10^{-6}e^{i108^\circ}\ \text{GeV}=1.05e^{-i14^\circ}E,$$
$$E_{\pi\pi}=1.3\times10^{-6}e^{i145^\circ}\ \text{GeV}=0.85e^{i23^\circ}E. \quad (29)$$

Using the input parameters for the light-cone distribution amplitudes of light mesons, quark masses and decay constants from Refs. [44,45] and form factors from Refs. [28,46],[2] we find

$$\left(\frac{P^s}{T+E}\right)_{\pi\pi}=0.35e^{-i175^\circ},\quad \left(\frac{P^d}{T+E}\right)_{KK}=0.24e^{-i176^\circ}. \quad (30)$$

Hence, $\delta_{\pi\pi}\approx\delta_{KK}=-176^\circ$. From Eqs. (25) and (26), we derive $a_{\rm dir}^{\rm t+p}(\pi^+\pi^-)=-3.9\times10^{-5}$ and $a_{\rm dir}^{\rm t+p}(K^+K^-)=2.0\times10^{-5}$, where $a_{\rm dir}^{\rm t+p}$ denotes the *CP* asymmetry arising from the interference between tree and QCD-penguin amplitudes. QCD-penguin induced *CP* asymmetries in $D^0\to\pi^+\pi^-$, K^+K^- are small partially due to the almost trivial strong phases of $\delta_{\pi\pi}$ and δ_{KK}.

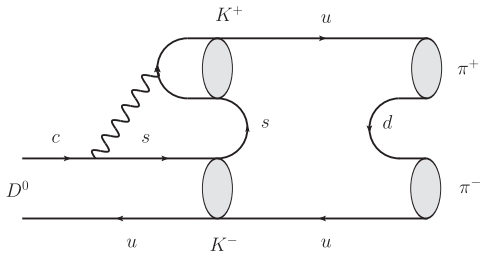

FIG. 2. Long-distance contribution to $D^0\to\pi^+\pi^-$ through a resonantlike final-state rescattering. It has the same topology as the QCD-penguin exchange topological diagram *PE*.

Short-distance weak penguin annihilation contributions (*PE* and *PA*) to charm decays are very small; typically, PE/T and PA/T are of order 10^{-5} and hence are negligible. Nevertheless, long-distance contributions to SCS decays, for example, $D^0\to\pi^+\pi^-$, can proceed through the weak decay $D^0\to K^+K^-$ followed by a resonantlike final-state rescattering as depicted in Fig. 2. It has the same topology as the QCD-penguin exchange topological graph *PE*. Just as the weak annihilation topologies *E* and *A*, it is expected that weak penguin annihilation will receive sizable long-distance contributions from final-state interactions as well. Recall that soft corrections due to penguin annihilation have been proposed to resolve some problems in hadronic *B* decays, for example, the rate deficit problem for penguin-dominated decays and the *CP* puzzle for $\bar B^0\to K^-\pi^+$ [35]. Hence, we shall assume that *PE*, PE_P, and PE_V are of the same order of magnitude as *E*, E_P, and E_V, respectively. For concreteness, we take (in units of 10^{-6})

$$PE=1.6e^{i115^\circ}\ \text{GeV},\quad PE_P=3.1e^{-i90^\circ},\quad PE_V=1.5e^{-i120^\circ}. \quad (31)$$

C. Numerical results and discussion

The calculated direct *CP* asymmetries for various SCS $D\to PP$ and $D\to VP$ decays are summarized in Table III.[3] Before embarking on *CP* violation, we have

[2]More specifically, we use $f_D=219$ MeV and $f_{D_s}=260$ MeV [45] for the charmed meson decay constants and those in [46] for $D\to V$ transition form factors.

[3]*CP*-violating asymmetries in SCS decays of charmed mesons have also been investigated in Ref. [48]. In this work, final-state interaction effects are studied by assuming that FSI's are dominated by nearby resonances, similar to the work of Refs. [32,34]. The major uncertainties there arise from the unknown masses and widths of the resonances at energies near the charmed meson mass. Noticeable differences between Ref. [48] and our results for direct *CP* asymmetries are that $\Delta a_{CP}^{\rm dir}$ of $D^0\to K^{*+}K^-$ and $D^0\to K^{*-}K^+$ are predicted to have the same sign in Ref. [48] and likewise for $D^0\to K^+K^-$ and $D^0\to\pi^+\pi^-$, whereas they are of opposite signs in our work.

TABLE III. Predictions of direct CP asymmetries in units of 10^{-3}, where $a_{\rm dir}^{\rm (tree)}$ denotes CP asymmetry arising from tree amplitudes. The superscript (t + p) denotes tree plus QCD-penguin amplitudes, (t + pa) for tree plus weak penguin-annihilation (PE and PA) amplitudes and "tot" for the total amplitude. For the VP modes, we use the solutions (A) and (A1) given in Eq. (8) for tree and weak annihilation amplitudes. For weak penguin annihilation, we assume that it is similar to the topological E amplitude [see Eq. (31)]. World averages of experimental measurements are taken from Ref. [3]. Because of the lack of information on the topological amplitudes A_P and A_V, no prediction is attempted for $D^+ \to VP$ and $D_s^+ \to VP$ decays.

Decay Mode	$a_{\rm dir}^{\rm (tree)}$	$a_{\rm dir}^{\rm (t+p)}$	$a_{\rm dir}^{\rm (t+pa)}$	$a_{\rm dir}^{\rm (tot)}$	Expt (10^{-3})	Decay Mode	$a_{\rm dir}^{\rm (tree)}$	$a_{\rm dir}^{\rm (t+p)}$	$a_{\rm dir}^{\rm (t+pa)}$	$a_{\rm dir}^{\rm (tot)}$
$D^0 \to \pi^+\pi^-$	0	-0.04	0.90	0.86	2.0 ± 2.2	$D^0 \to \pi^+\rho^-$	0	0.10	-0.60	-0.51
$D^0 \to \pi^0\pi^0$	0	0.25	0.59	0.85	1 ± 48	$D^0 \to \pi^-\rho^+$	0	-0.05	-0.22	-0.27
$D^0 \to \pi^0\eta$	0.63	0.43	0.03	-0.16		$D^0 \to \pi^0\rho^0$	0	0	-0.74	-0.74
$D^0 \to \pi^0\eta'$	-0.51	-0.60	0.09	-0.01		$D^0 \to K^+K^{*-}$	0	-0.10	0.60	0.50
$D^0 \to \eta\eta$	-0.37	-0.38	-0.70	-0.71		$D^0 \to K^-K^{*+}$	0	0.06	0.22	0.29
$D^0 \to \eta\eta'$	0.39	0.44	0.21	0.25		$D^0 \to K^0\bar{K}^{*0}$	0.73	0.73	0.73	0.73
$D^0 \to K^+K^-$	0	0.02	-0.50	-0.48	-2.3 ± 1.7	$D^0 \to \bar{K}^0K^{*0}$	-0.73	-0.73	-0.73	-0.73
$D^+ \to \pi^+\pi^0$	0	0	0	0		$D^0 \to \pi^0\omega$	0	-0.15	0.53	0.37
$D^+ \to \pi^+\eta$	0.37	0.28	-0.56	-0.65	17.4 ± 11.5[a]	$D^0 \to \pi^0\phi$	0	0	0	0
$D^+ \to \pi^+\eta'$	-0.21	-0.26	0.42	0.41	-1.2 ± 11.3[a]	$D^0 \to \eta\omega$	0.19	0.19	0.50	0.50
$D^+ \to K^+\bar{K}^0$	-0.07	0.08	-0.53	-0.38	-0.9 ± 6.3	$D^0 \to \eta'\omega$	-1.07	-1.05	-0.91	-0.89
$D_s^+ \to \pi^+K^0$	0.09	-0.07	0.69	0.52	65.3 ± 24.6	$D^0 \to \eta\phi$	0	0	0	0
$D_s^+ \to \pi^0K^+$	0.01	0.02	0.87	0.88	20 ± 290	$D^0 \to \eta\rho^0$	-0.53	-0.54	-0.22	-0.23
$D_s^+ \to K^+\eta$	-0.61	-0.27	-0.53	-0.19	-200 ± 180	$D^0 \to \eta'\rho^0$	0.59	0.58	0.21	0.20
$D_s^+ \to K^+\eta'$	0.35	0.58	-0.63	-0.41	-170 ± 370					

[a]Data from [47].

taken into account the SU(3) breaking effects in tree amplitudes T and C using the factorization approach so that the predicted branching fractions are consistent with the data shown in Tables I and II. Besides the aforementioned example for $D^0 \to \pi^+\pi^-$ and $D^0 \to K^+K^-$, we found, for example, $T_{\pi^+\eta^{(\prime)}}/T = 0.85$, $C_{\pi^+\eta^{(\prime)}}/C = 0.93$ for the decays $D^+ \to \pi^+\eta^{(\prime)}$ [28]. The predicted branching fractions $\mathcal{B}(D^+ \to \pi^+\eta) = (3.02 \pm 0.19) \times 10^{-3}$ and $\mathcal{B}(D^+ \to \pi^+\eta') = (4.69 \pm 0.21) \times 10^{-3}$ with $A_{\pi^+\eta^{(\prime)}}/A = 0.7$ are in agreement with the measured ones $\mathcal{B}(D^+ \to \pi^+\eta) = (3.53 \pm 0.21) \times 10^{-3}$ and $\mathcal{B}(D^+ \to \pi^+\eta') = (4.67 \pm 0.29) \times 10^{-3}$ (see Table I).

In general, tree-level CP violation lies in the range $10^{-4} < a_{\rm dir}^{\rm (tree)} < 10^{-3}$. The largest one occurs in the decay $D^0 \to \omega\eta'$ where $a_{\rm dir}^{\rm (tree)} = -1.1 \times 10^{-3}$. We would like to accentuate once again that the estimation of tree-level CP asymmetries in the diagrammatic approach is reliable and trustworthy since the magnitude and phase of the tree topological amplitudes are extracted from the measured data. By an inspection of $a_{\rm dir}^{\rm (tree)}$, one can get an idea about the size of direct CP violation within the SM.

The QCD-penguin effects on CP asymmetry can be inferred from a comparison between $a_{\rm dir}^{\rm (t+p)}$ and $a_{\rm dir}^{\rm (tree)}$. We see from Table III that the short-distance penguin effects are small compared to the tree-amplitude-induced CP violation. For decay modes with vanishing $a_{\rm dir}^{\rm (tree)}$, the QCD-penguin induced CP asymmetry is of order (1–2) $\times$ 10^{-4} or even smaller (see Table III).

When the short-distance weak penguin annihilation contribution is estimated in QCDF at the hard-collinear scale $\mu_h \approx 800$ MeV, it is found to be very small as mentioned before. But weak penguin annihilation has the chance to be greatly enhanced. In QCDF, it involves endpoint divergences related to the soft gluon effects. In the diagrammatic approach, it receives long-distance contributions from the color-allowed tree amplitude followed by final-state rescattering as shown in Fig. 2. Assuming that penguin annihilation is similar to the topological W-exchange amplitude [see Eq. (31)], its effect can be studied by comparing $a_{\rm dir}^{\rm (t+pa)}$ with $a_{\rm dir}^{\rm (tree)}$, where the superscript "pa" denotes weak penguin annihilation. It is evident from Table III that penguin annihilation could play an essential role in the study of CP violation.

After summing over all possible contributions, we see that the predicted CP violation denoted by $a_{CP}^{\rm tot}$ (or $a_{CP}^{\rm dir}$) is at most of order 10^{-3} in the SM. For $\Delta a_{CP}^{\rm dir}$, the CP asymmetry difference in $D^0 \to K^+K^-$ and $D^0 \to \pi^+\pi^-$, we obtain a value of -0.13%, which is too small compared to the world average of $-(0.645 \pm 0.180)\%$. Since in the SM, $\Delta a_{CP}^{\rm dir}$ stems mainly from weak penguin annihilation, we can vary the amplitude PE to see how much enhancement we can gain. Even with the maximal magnitude $|PE| \sim T$ and a maximal strong phase relative to T, we get $\Delta a_{CP}^{\rm dir} = -0.25\%$. This is more than 2σ away from the current world average. Hence, if the LHCb result for $\Delta a_{CP}^{\rm dir}$ is confirmed by further data analysis, it will imply new physics in the charm sector.

V. CONCLUSIONS

In view of the recently measured CP asymmetry difference $\Delta a_{CP}^{\rm dir}$ between the $D^0 \to K^+K^-$ and $D^0 \to \pi^+\pi^-$ modes, we scrutinize the direct CP violation in the singly Cabibbo-suppressed (SCS) $D \to PP$ and VP decays within the standard model (SM), where P and V refer to pseudoscalar and vector mesons, respectively. Such an analysis is helpful in diagnosing possible evidence of new physics in the charm sector.

Direct CP violation in such D decays may arise from the interference between tree-level amplitudes of different topologies. However, the magnitude is proportional to $\mathrm{Im}(V_{cd}^* V_{ud} V_{cs}^* V_{us})/|V_{cd}^* V_{ud}|^2$, which is $\mathcal{O}(10^{-3})$. Modulated by the size ratio of different flavor amplitudes and the sine of the relative strong phase, we expect that such tree-level CP asymmetry should be at the order of 10^{-3} or even smaller. The great merit of the topological approach is that the magnitude and the relative strong phase of each individual topological tree amplitude in charm decays can be extracted from the data. Hence, the estimate of $a_{CP}^{\rm dir}$ should be trustworthy and reliable. We find that $a_{CP}^{\rm dir}(D^0 \to \omega\eta') \sim -1.1 \times 10^{-3}$ is the largest one among all the SCS modes.

In the $D^0 \to K^+K^-$ and $D^0 \to \pi^+\pi^-$ decays, the tree-level amplitudes have exactly the same CKM factors and thus do not induce direct CP asymmetry. In such cases, one must invoke the penguin amplitudes, including the QCD penguin and weak penguin annihilation amplitudes. In addition, we have taken into account the SU(3) breaking effects in the color-allowed tree T diagram and the resonance effects in W-exchange E diagram, as done in Ref. [28], in order to explain the observed branching fractions of the two modes. As given in the $a_{\rm dir}^{(\rm t+p)}$ column of Table III, the direct CP asymmetries of both modes are at a few $\times 10^{-5}$ level. This is seen to be largely due to the trivial relative strong phase between the QCD-penguin amplitude and the tree-level amplitudes.

We next include the contributions of weak penguin annihilation diagrams, PE, PE_P, and PE_V. The short-distance contributions of such diagrams are typically 5 orders of magnitude smaller than the color-allowed tree diagram and thus negligible. However, they may be enhanced by long-distance final-state rescattering through resonances, as in the case of the weak annihilation diagrams E and A. We manage to maximize the CP -violating effects from the interference with these weak penguin annihilation diagrams by assuming these diagrams are as large as the tree-level E, E_P, and E_V, respectively, and have sizable strong phases relative to T. In the end, we observe that the magnitude of CP asymmetry in the SCS charm decay modes can reach at most 10^{-3}. In particular, the CP asymmetry difference $\Delta a_{CP}^{\rm did}$ between $D^0 \to K^+K^-$ and $D^0 \to \pi^+\pi^-$ is found to be about -0.13%. Even with the parameter choices of $|PE| \sim |T|$ and a relative strong phase of 90°, we find $\Delta a_{CP}^{\rm dir} = -0.25\%$, which can be regarded as the upper bound on $\Delta a_{CP}^{\rm dir}$ in the SM, still more than 2σ away from the world-average experimental result $-(0.645 \pm 0.180)\%$.

In conclusion, if $\Delta a_{CP}^{\rm dir}$ continues to be large with more statistics in the future or if the direct CP asymmetry of any of the discussed modes is significantly larger than 10^{-3}, it will be clear evidence of physics beyond the SM in the charm sector.

ACKNOWLEDGMENTS

This research was supported in part by the National Science Council of Taiwan, Republic Of China, under Grant Nos. NSC-100-2112-M-001-009-MY3 and NSC-100-2628-M-008-003-MY4 and in part by the NCTS.

[1] R. Aaij *et al.* (LHCb Collaboration), Phys. Rev. Lett. (to be published).
[2] T. Aaltonen *et al.* (CDF Collaboration), Phys. Rev. D **85**, 012009 (2012).
[3] D. Asner *et al.* (Heavy Flavor Averaging Group), arXiv:1010.1589 and online update at http://www.slac.stanford.edu/xorg/hfag.
[4] C. Quigg, Z. Phys. C **4**, 55 (1980).
[5] M. Golden and B. Grinstein, Phys. Lett. B **222**, 501 (1989).
[6] I. Hinchliffe and T. A. Kaeding, Phys. Rev. D **54**, 914 (1996).
[7] G. Isidori, J. F. Kamenik, Z. Ligeti, and G. Perez, arXiv:1111.4987.
[8] J. Brod, A. L. Kagan, and J. Zupan, arXiv:1111.5000.
[9] K. Wang and G. Zhu, arXiv:1111.5196.
[10] A. N. Rozanov and M. I. Vysotsky, arXiv:1111.6949.
[11] Y. Hochberg and Y. Nir, arXiv:1112.5268;D. Pirktskhalava and P. Uttayarat, arXiv:1112.5451.
[12] I. I. Bigi and A. Paul, arXiv:1110.2862.
[13] I. I. Bigi, A. Paul, and S. Recksiegel, J. High Energy Phys. 06 (2011) 089.
[14] M. Beneke, G. Buchalla, M. Neubert, and C. T. Sachrajda, Phys. Rev. Lett. **83**, 1914 (1999); Nucl. Phys. B **591**, 313 (2000).
[15] Y. Y. Keum, H. N. Li, and A. I. Sanda, Phys. Rev. D **63**, 054008 (2001).
[16] C. W. Bauer, D. Pirjol, I. Z. Rothstein, and I. W. Stewart, Phys. Rev. D **70**, 054015 (2004).
[17] H. Y. Cheng and C. K. Chua, Phys. Rev. D **80**, 114008 (2009); **80**, 074031 (2009).
[18] H. Y. Cheng, Phys. Rev. D **26**, 143 (1982); A. Datta and D. Kumbhakar, Z. Phys. C **27**, 515 (1985).

[19] M. Bobrowski, A. Lenz, J. Riedl, and J. Rohrwild, J. High Energy Phys. 03 (2010) 009.
[20] A. F. Falk, Y. Grossman, Z. Ligeti, and A. A. Petrov, Phys. Rev. D **65**, 054034 (2002).
[21] H. Y. Cheng and C. W. Chiang, Phys. Rev. D **81**, 114020 (2010).
[22] L. L. Chau Wang, in *AIP Conference Proceedings 72 (1980), Weak Interactions as Probes of Unification*, edited by G. B. Collins, L. N. Chang, and J. R. Ficenec (AIP, New York, 1981), p. 419–431; in *Proceedings of the 1980 Guangzhou Conference on Theoretical Particle Physics* (Science Press, Beijing, China, 1980), p.1218; L. L. Chau, Phys. Rep. **95**, 1 (1983).
[23] L. L. Chau and H. Y. Cheng, Phys. Rev. Lett. **56**, 1655 (1986).
[24] L. L. Chau and H. Y. Cheng, Phys. Rev. D **36**, 137 (1987); Phys. Lett. B **222**, 285 (1989).
[25] H. Y. Cheng and S. Oh, J. High Energy Phys. 09 (2011) 024.
[26] K. Nakamura *et al.* (Particle Data Group), J. Phys. G **37**, 075021 (2010).
[27] R. Kass, talk presented at *2009 Europhysics Conference on High Energy Physics* (Krakow, Poland, 2009).
[28] H. Y. Cheng and C. W. Chiang, Phys. Rev. D **81**, 074021 (2010).
[29] B. Bhattacharya and J. L. Rosner, Phys. Rev. D **77**, 114020 (2008).
[30] F. Ambrosino *et al.*, J. High Energy Phys. 07 (2009) 105.
[31] B. Bhattacharya and J. L. Rosner, Phys. Rev. D **79**, 034016 (2009).
[32] P. Żenczykowski, Acta Phys. Pol. B **28**, 1605 (1997).
[33] S. Weinberg, *The Quantum Theory of Fields, Volume I* (Cambridge University Press, New York, 1995), Sec. 3.8.
[34] H. Y. Cheng, Eur. Phys. J. C **26**, 551 (2003).
[35] M. Beneke and M. Neubert, Nucl. Phys. **B675**, 333 (2003).
[36] M. Wirbel, B. Stech, and M. Bauer, Z. Phys. C **29**, 637 (1985); M. Bauer, B. Stech, and M. Wirbel, *ibid.* **34**, 103 (1987).
[37] H.-n. Li and B. Tseng, Phys. Rev. D **57**, 443 (1998); D. S. Du, Y. Li, and C. D. Lu, Chin. Phys. Lett. **23**, 2038 (2006).
[38] H. J. Gong, J. F. Sun, and D. S. Du, High Energy Phys. Nucl. Phys. **26**, 665 (2002).
[39] X. Y. Wu, X. G. Yin, D. B. Chen, Y. Q. Guo, and Y. Zeng, Mod. Phys. Lett. A **19**, 1623 (2004); X. Y. Wu, X. G. Yin, and Y. Q. Guo, Chin. Phys. **13**, 469 (2004); X. Y. Wu, B. J. Zhang, H. B. Li, X. J. Liu, B. Liu, J. W. Li, and Y. Q. Guo, Phys. Lett. B **675**, 196 (2009).
[40] J. H. Lai and K. C. Yang, Phys. Rev. D **72**, 096001 (2005).
[41] D. N. Gao, Phys. Lett. B **645**, 59 (2007).
[42] Y. Grossman, A. L. Kagan, and Y. Nir, Phys. Rev. D **75**, 036008 (2007).
[43] L. L. Chau and H. Y. Cheng, Phys. Rev. Lett. **53**, 1037 (1984).
[44] H. Y. Cheng and C. K. Chua, Phys. Rev. D **80**, 114008 (2009).
[45] A. Bazavov, C. Bernard, C. M. Bouchard, C. DeTar, M. Di Pierro, A. X. El-Khadra, R. T. Evans, and E. D. Freeland *et al.*, arXiv:1112.3051.
[46] Y. L. Wu, M. Zhong, and Y. B. Zuo, Int. J. Mod. Phys. A **21**, 6125 (2006).
[47] E. Won *et al.* (Belle Collaboration), Phys. Rev. Lett. **107**, 221801 (2011).
[48] F. Buccella, M. Lusignoli, G. Miele, A. Pugliese, and P. Santorelli, Phys. Rev. D **51**, 3478 (1995).